uc3m | Universidad **Carlos III** de Madrid
Escuela Politécnica Superior

Diffusion-driven growth and dissolution of quasi-static bubbles

Tesis Doctoral

Autor:
PABLO PEÑAS LÓPEZ

Director:
JAVIER RODRÍGUEZ RODRÍGUEZ

Codirector:
MIGUEL ÁNGEL PARRALES BORRERO

DEPARTAMENTO DE INGENIERÍA TÉRMICA Y DE FLUIDOS

Leganés, Noviembre 2017

uc3m

Tesis Doctoral

Diffusion-driven growth and dissolution
of quasi-static bubbles

Autor: Pablo Peñas López

Director de Tesis: Javier Rodríguez Rodríguez

Codirector de Tesis: Miguel Ángel Parrales Borrero

Firma del Tribunal Calificador:

Firma

Presidente: Dr. -

Vocal: Dr. -

Secretario: Dr. -

Suplente: Dr. -

Calificación:

Leganés, – de Noviembre de 2017

To my parents, Gabriel & Mariajosé

*Knowledge is of two kinds. We know a subject ourselves,
or we know where we can find information upon it.*

– Samuel Johnson (1709–1784)

There is no angry way to say "bubbles".

– Author Unknown

Abstract

Growing or dissolving bubbles are present in countless mass transfer processes that involve liquid and gas phases. This thesis comprises the fundamental study of four distinct but closely related problems concerning the diffusion-driven dissolution and growth of quasi-static gas bubbles. The term 'quasi-static' loosely describes the condition under which advection effects contribute poorly to the the rate of growth or dissolution of the bubble; 'diffusion-driven' indicates that mass transfer is governed by the solute diffusion in the surrounding bulk liquid. In super- or under-saturated solutions, diffusion effects are critical in the growth or dissolution behaviour of bubbles adhered to substrates including gas-evolving electrodes, and of bubbles in viscoelastic gels or under confinement, to name but a few examples.

We first explore the dissolution of mm-sized CO_2 spherical cap bubbles immersed in air-saturated water and adhered to collagen-coated glass and PMMA substrates. We validate a theoretical and numerical model against our experiments. Both account for the relevant influence of the contact angle dynamics and presence of the substrate on mass transfer across the bubble interface.

We then focus on the study of the so-called 'history effect', namely the contribution of any past mass transfer events between a gas bubble and its liquid surroundings towards the current bubble growth or dissolution rate. The history effect arises when the concentration of dissolved gas at the bubble surface, dictated by Henry's law, depends on time. Firstly, we provide a theoretical treatment of the history effect under the assumptions of spherical symmetry and negligible advection. Secondly, we perform experiments on isolated spherical CO_2 bubbles adhered to a flat plate in carbonated water. This configuration was chosen for being closer to several practical applications. Additionally, we perform simulations to quantify the importance of the history effect versus the effects of boundary-induced advection and density-induced natural convection on the bubble dynamics.

The third scenario entails the dissolution of a cylindrical CO_2 bubble confined in a horizontal Hele-Shaw cell dissolving in air-saturated water. We visualize and track, by means of planar laser-induced fluorescence, the boundary layer of dissolved CO_2 that propagates by diffusion from the dissolving bubble. The diffusion-driven transport of CO_2 are then described by two simple analytical diffusion models which are then validated against numerical simulations. Finally, the fluorescence intensity profiles are related to the expected CO_2 concentration and pH profiles.

The fourth and final study is centred on the growth dynamics of a succession of H_2 bubbles under constant-current electrolysis. The bubbles nucleate and grow on a micropillar protruding from an otherwise flat silicon electrode. The accumulation of dissolved H_2 near the gas-evolving electrode is hindered by several depletion sources, including depletion from previous bubbles in the succession. The degree of supersaturation near the electrode, and consequently the bubble growth rates, are found to be largely unsteady and prone to fluctuations. Moreover, depletion effects (e.g. from parasitic bubbles growing nearby) are responsible for a notable retardation in the growth rate as the bubbles approached their departure size.

Resumen

Incontables procesos de transferencia de masa entre fases líquidas y gaseosas cuentan con la presencia de burbujas que crecen o se disuelven. Esta tesis engloba el estudio fundamental de cuatro problemas distintos sobre el crecimiento o la disolución por difusión de burbujas cuasi-estáticas. El término "cuasi-estático" describe de manera genérica la condición bajo la cual los efectos convectivos contribuyen de forma escasa al ritmo de crecimiento o disolución de la burbuja; "por difusión" indica que la transferencia de masa está siendo gobernada por la difusión del gas disuelto en el líquido que rodea la burbuja. En disoluciones sobre- o sub-saturadas, los efectos difusivos son críticos en el comportamiento de crecimiento o disolución de burbujas adheridas a sustratos incluyendo electrodos que evolucionan gas, y de burbujas en geles viscoelásticos o en confinamiento, por ejemplo.

Primero exploramos la disolución de burbujas de CO_2 con forma de casquete esférico (de tamaño milimétrico) inmersas en agua saturada de aire y adheridas a placas de cristal o PMMA. Validamos un modelo teórico y numérico contra nuestros experimentos. Ambos tienen en cuenta el efecto influyente de la dinámica de la línea de contacto y la presencia de la placa en la transferencia de masa a través de la interfaz de la burbuja.

Después nos centramos en el estudio del llamado 'efecto de historia', concretamente la contribución que los eventos pasados de transferencia de masa entre el líquido y la burbuja tienen en el ritmo actual de crecimiento o disolución de la burbuja. El efecto de historia surge cuando la concentración del gas soluto en la superficie de la burbuja, dictada por la ley de Henry, depende en el tiempo. En primer lugar presentamos un tratamiento teórico del efecto de historia bajo las hipótesis de simetría esférica y advección despreciable. En segundo lugar, realizamos experimentos en burbujas esféricas de CO_2 adheridas a una placa plana en agua carbonatada. Adicionalmente, hacemos simulaciones para cuantificar el efecto de historia en la dinámica de las burbujas junto a los efectos de la advección inducida por la superficie no estacionaria de la burbuja y por convección natural.

El tercer escenario consiste en la disolución de una burbuja cilíndrica de CO_2 confinada en una celda Hele-Shaw horizontal en agua saturada de aire. Visualizamos y registramos, mediante fluorescencia inducida por láser, la capa límite de CO_2 disuelto que se propaga por difusión desde la burbuja. Seguidamente, describimos el transporte por difusión de CO_2 mediante dos sencillos modelos analíticos que son posteriormente validados frente a simulaciones numéricas. Finalmente, mostramos la relación del perfil de intensidad de fluorescencia con los perfiles de concentración de CO_2 y de pH calculados.

El cuarto y último estudio se centra en la dinámica de crecimiento de una sucesión de burbujas de H_2 producidas mediante electrólisis a intensidad de corriente eléctrica constante. Las burbujas nuclean y crecen en un micro-pilar fabricado sobre un electrodo de silicio plano. La acumulación del hidrógeno disuelto cerca del electrodo es ralentizada por varias fuentes de pérdida de gas, en las que se incluye las pérdidas inducidas por las propias burbujas. El grado de sobresaturación cerca del electrodo, y consecuentemente el ritmo de crecimiento de las burbujas, son altamente inconstantes y propensos a fluctuar. Además, las pérdidas (debido, por ejemplo, a la formación cercana de burbujas parasíticas) son responsables de un notable enlentecimiento en el ritmo de crecimiento a medida que las burbujas van alcanzando el tamaño de desprendimiento.

Contents

Introduction

1.1 Growing and dissolving bubbles

Growing or dissolving bubbles are present in countless mass transfer processes –whether man-made or in nature – that involve liquid and gas phases. Gas bubbles are observed to grow in subsurface porous media during oil extraction (Akin & Kovscek, 2002), on (micro)electrodes during water electrolysis (Chandran *et al.*, 2015; Yang *et al.*, 2015), in the eruptive degassing of volcanic magma (Mangan *et al.*, 2004), in the breaking of ocean surface waves (Couder, 2012), or as they rise in a glass of champagne (Liger-Belair, 2005). Bubble swarms are forced to dissolve in solvents in industrial bubble column reactors (Kantarci *et al.*, 2005) in many chemical processes, including chlorination or the postcombustion capture process of CO_2 (Haszeldine, 2009). In microfluidics, the dissolution of bubbles forms the basis of multiphase microchemical reactors (de Mas *et al.*, 2003), and it likewise represents a critical step in the manufacture of stable coated microbubbles (Park *et al.*, 2010) for biomedical applications.

Bubbles, however, are not always welcome. Cavitation bubbles and propellers aside (Carlton, 2012), the nucleation and growth of gas bubbles can be detrimental in some situations, including in microfluidic environments (Volk *et al.*, 2015), in the arteries or tissue of divers and pilots after decompression (Papadopoulou *et al.*, 2013), or during the molding process of polymer melts (Kontopoulou & Vlachopoulos, 1999).

Despite the evident diversity and complexity of the processes in which bubbles may grow or dissolve, all of them share the unequivocal phenomenon of mass transfer between the bubbles and their liquid surroundings. A diffusion flux of at least one soluble gas [e.g. air (N_2, O_2), CO_2, or H_2] and/or vapour species must occur from the bubble to the liquid, or vice versa. The liquid medium is often termed 'liquid–gas solution', precisely because it contains dissolved gas.

In truth, all bubbles have both gas (assumed noncondensable) and vapour content in variable amounts depending on the conditions under which they are found. Nonetheless, it is common practice to separate bubbles, including cavitation bubbles, into two kinds according to their composition (Plesset & Prosperetti, 1977). The first kind comprises gas or gaseous bubbles, i.e. those which are predominantly of noncondensable gas content; the second kind comprises vapour or vaporous bubbles, which are composed predominantly of the vapour of the surrounding liquid. Most of the examples given above belong to the first kind, whereas bubbles produced in superheated liquid mediums (boiling) and/or under strong acoustic forcing are likely to be mostly vaporous.

In many situations, however, the co-existence of the vapour and gas species must be taken into consideration in order to properly explain or model the dynamics of bubble growth or dissolution. For instance, bubble growth due to plasmonic heating is governed by the vaporisation of water only during the initial tenth of a second, to be subsequently controlled by the uptake of dissolved air from the surrounding water (Wang *et al.*, 2017). In PDMS devices permeable to gases, the vapour pressure of the liquid plays an important role in the stability of air bubbles (Volk *et al.*, 2015). Shpak *et al.* (2013) highlight the fundamental role of gas diffusion in preventing the total collapse of ultrasonically-driven (cavitating) vapour bubbles in a superheated liquid, a role also exhibited by argon gas in single-bubble sonoluminescence (Brenner *et al.*, 2002).

The work contained in the main chapters of this thesis strictly concerns bubbles of the first kind, i.e. bubbles which are assumed to be composed of a single or a mixture of noncondensable gases. The vapour pressure is sufficiently small as to neglect all the vapour content. In the discussion that follows we make no exception. We find it pertinent to briefly introduce, with some formalism, some elemental but essential concepts of mass transfer regarding gas bubbles in liquid–gas solutions.

1.2   Some fundamental notions

It is no surprise that the problem formulation of bubble dynamics and mass transfer is incredibly complex. Formally, one would need to consider the conservation equations of mass, species, momentum, and energy both in the gas and in the liquid, together with the appropriate balances at the bubble–liquid interface. Fortunately, the physics of a particular problem can be well captured by simplifying the general formulation through a series of approximations (Hsieh, 1965). Historically, all theoretical treatments of bubble growth or dissolution in unbounded liquids has been based upon the godly assumption of spherical symmetry. In other words, or rather in the words of Prosperetti (1982), spherical symmetry implies that the bubble is an "[isolated] spherical cavity, the centre of which is fixed [i.e. at rest] in an unbounded incompressible viscous liquid free of body forces". A second simplification, employed in no lesser extent, is the assumption of uniformity of the bubble interior. This led to the derivation of several approximate analytical solutions over half a century ago (Hsieh, 1965), some of which are still widely used to this day. These solutions consider the bubble growth dynamics dominated by a particular effect, namely by diffusion (Epstein & Plesset, 1950), rectified diffusion (Hsieh & Plesset, 1961), self-similar or asymptotic growth (Birkhoff *et al.*, 1958; Scriven, 1959), inertial effects, or thermal effects (Plesset & Zwick, 1954).

In a similar way, we proceed to illustrate the key ingredients in the physics of these problems from an introductory perspective. We choose to split the problem into two parts: we first focus on the bubble interior and then on the surrounding liquid–gas solution.

Inside the bubble

For the sake simplicity, we shall consider a spherical monocomponent bubble under the aforementioned assumption of spherical symmetry. In such a case, the bubble dynamics is governed by the classical Rayleigh–Plesset equation (Plesset & Prosperetti, 1977) or any of its variants, which relates any variation in the liquid far-field pressure $P_\infty(t)$ with the

dynamic response of the bubble radius $R(t)$. We choose to write a modified Rayleigh–Plesset equation that additionally accounts for mass transfer effects (Prosperetti, 1982; Fuster & Montel, 2015),

$$R\ddot{R} - \frac{R\dot{J}}{\rho_l} + \frac{3}{2}\left(\dot{R} - \frac{J}{\rho_l}\right)^2 - \frac{2J}{\rho_l}\left(\dot{R} - \frac{J}{\rho_l}\right) = \frac{1}{\rho_l}\left[P_g - \frac{2\gamma_{lg}}{R} - \frac{4\mu}{R}\left(\dot{R} - \frac{J}{\rho_l}\right) - P_\infty\right], \quad (1.1)$$

where $P_g(t)$ is the gas pressure acting on the inner side of the bubble interface, γ_{lg} is the surface tension, μ and ρ_l are the viscosity and density of the liquid, and $J(t)$ is the net mass flux across the infinitely thin interface into the bubble. Note the dot notation in place of d/dt.

To evaluate the radius dynamics $R(t)$ from (1.1), $P_g(t)$ must be known first. We proceed to invoke the assumption of uniformity of the bubble interior: the gas contents are assumed motionless and in equilibrium. The Mach number of the bubble wall, $Ma_g \sim \dot{R}(\rho_g/P_g)^{1/2}$, needs to be small. It can be shown (Prosperetti *et al.*, 1988) that the maximum pressure difference in the bubble can be neglected provided that $\Delta P_g/P_g \sim Ma_g^2 \ll 1$. Thus, in such cases, the gas pressure $P_g(t)$, temperature $T_g(t)$ and hence density $\rho_g(t)$ inside the bubble are uniform and are just functions of time. Then, it is possible to obtain $P_g(t)$ from an equation of state of the form

$$P_g = P_g(\rho_g, T_g), \quad (1.2)$$

examples being the van der Waals, polytropic gas or ideal gas equations of state. The density $\rho_g(t)$ is related to the mass flux $J(t)$ through a simple mass balance,

$$\frac{\mathrm{d}}{\mathrm{d}t}\left(\frac{4}{3}\pi R^3\rho_g\right) = 4\pi R^2 J \quad (1.3)$$

where the left-hand side is the rate of change of the bubble mass. The Rayleigh–Plesset equation is thus closed, provided that $J(t)$ is known at all times.

It is imperative to realize that the mass flux $J(t)$ acts on the Rayleigh–Plesset equation (1.1) through two channels. Firstly and most importantly, through the pressure $P_g(t)$. Secondly, through the inertial or viscous terms explicitly containing J and $\dot{J}$. While the the contribution of the first channel is paramount, it will be seen that the contribution of the second channel is, in most cases, negligible. In fact, the J- and $\dot{J}$-containing terms arise from the rather rigorous consideration that the radial liquid velocity adjacent to the bubble interface $U_l(t)$, must be different to the interface velocity $\dot{R}(t)$ for the case of mass transfer, $J(t) \neq 0$. The velocity difference causes a mass flow rate $4\pi R^2\rho_l(\dot{R} - U_l)$ which must just equal the rate of exsolution of soluble material into the bubble. Mass balance across the interface gives (Scriven, 1959; Hsieh, 1965)

$$J = \rho_l(\dot{R} - U_l). \quad (1.4)$$

Setting $J = \dot{J} = 0$ explicitly in the Rayleigh–Plesset equation (1.1) is strictly equivalent to making the approximation that the liquid velocity at the interface is equal to the interface velocity, $U_l = \dot{R}$. In doing so, one neglects the presumably small contribution of the second channel, namely the effect of this small velocity difference on the inertial and viscous terms. The classical Rayleigh–Plesset equation is thereby recovered. This approximation is often justified since, as noted by Scriven (1959), during bubble growth or dissolution the volume can vary by orders of magnitude but the gas density changes relatively little. Hence, substituting (1.3) in (1.4) and assuming, just for this purpose, that ρ_g is independent of time,

one gets that $U_l/\dot{R} = 1 - \rho_g/\rho_l$. Given that typically $\rho_g/\rho_l \sim 10^{-3}$, it is permissible to assume that $U_l = \dot{R}$ for the majority of bubble mass transfer problems. This assumption will be also made throughout the remainder of this thesis.

Before moving on, we wish to close off this discussion by addressing the fundamental notion that a gas bubble momentarily grows or shrinks (exclusively as a consequence of mass transfer) according to the quantity represented by right-hand side of (1.3), i.e. the net mass flow rate across the bubble interface at a given time. Simply put, the bubble grows as long as $J > 0$; if $J < 0$ the bubble dissolves, whereas if $J = 0$ the bubble mass remains constant. One must not confuse pressure-induced compression or expansion with dissolution or growth. For instance, consider an insoluble gas bubble ($J = 0$ always and everywhere) that is suddenly subjected to a step increase in ambient pressure $P_\infty(t)$. The gas bubble must then compress according to the equation of state (1.2) and the dynamical equation (1.1), and its volume will surely experience a sudden shrinkage. Similarly, a step decrease in pressure will cause the bubble to expand. The mass of the bubble, on the other hand, remains unaltered. It follows that, for these cases in which bubbles grow and dissolve under time-dependent ambient pressures (Jones & Zuber, 1978; Payvar, 1987), compressibility and mass transfer simultaneously contribute to any variations in the bubble volume. Sometimes it is desirable to quantify the volume variations purely due to mass transfer. In such a case, the bubble volume must be pressure-corrected first (§§ 3–4 of this thesis)

Outside the bubble

The remaining piece of the problem, from which the net mass flux $J(t)$ can be evaluated, amounts to solving for the spatio-temporal evolution of the concentration field of the dissolved gas species in the liquid–gas solution surrounding the bubble. The boundary conditions for the liquid velocity and concentration of dissolved species and at the interface depend, of course, on the bubble interface velocity and bubble contents (namely the partial pressures) at that particular instant of time.

Returning to our idealised example of a monocomponent translationless bubble under spherical symmetry, let $C(r, t)$ denote the mass-based concentration field (often referred to as density) of the gas species dissolved in the liquid, where r is the radial distance from the bubble centre. The transport of dissolved gas species in the liquid is then governed by the following mass balance equation, usually termed advection–diffusion equation,

$$\frac{\partial C}{\partial t} + U(r, t)\frac{\partial C}{\partial r} = D\frac{1}{r^2}\frac{\partial}{\partial r}\left(r^2\frac{\partial C}{\partial r}\right), \tag{1.5}$$

where D is the gas diffusion coefficient in the liquid. By virtue of the continuity equation, we obtain the radial velocity field $U(r, t) = U_l R^2/r^2 \cong \dot{R}R^2/r^2$ that is induced purely by the rate of change of the bubble radius. The mass flux (into the bubble) across the bubble interface is dictated by the concentration gradient evaluated at the interface, as stated by Fick's first law:

$$J(t) = (\dot{R} - U_l)C(R, t) + D\left.\frac{\partial C}{\partial r}\right|_{r=R(t)} \cong D\left.\frac{\partial C}{\partial r}\right|_{r=R(t)}. \tag{1.6}$$

As discussed above, the advective or bulk flux term is usually negligible in comparison to the diffusion flux. Upon the very valid assumption that $U_l = \dot{R}$, the bulk flux term formally disappears.

Finally, two boundary conditions are required to evolve (1.5) in time. The first is the far-field concentration, $C(r \to \infty, t) = C_\infty$, which is usually a known constant. The second is the so-called interfacial concentration, i.e. the concentration of dissolved gas in the liquid immediately adjacent to the bubble interface. The interfacial concentration is assumed to be equal to the equilibrium or saturation concentration, $C(R, t) = C_s(t)$, at all times. The saturation or equilibrium concentration is in fact proportional to the partial pressure of the gas acting on the liquid surface,

$$C_s(t) = k_H P_g(t), \tag{1.7}$$

as stated by Henry's law. Henry's constant k_H is a decreasing function of temperature specific to each liquid–gas pair. Note that the uniformity condition of the bubble interior implies that $P_g(t)$ in (1.7) is simply the partial pressure of the gas in the bubble.

Let us now consider a liquid–gas solution (containing a single gas species) of uniform gas concentration C_∞ and at ambient temperature T_∞ and pressure P_∞. Henry's law implies that the saturation concentration of the liquid in such conditions is $C_{sat} = k_H(T_\infty)P_\infty$. It stands to reason that reducing the temperature (thereby increasing the gas solubility k_H) or increasing the pressure increments the saturation concentration, i.e. the gas uptake capability by the liquid increases. Similarly, the saturation pressure of such a solution, i.e. the pressure at which the solution becomes saturated, is given by $P_{sat} = C_\infty/k_H(T_\infty)$, Therefore, a liquid solution is said to be supersaturated if $C_\infty > C_{sat}$ and $P_\infty < P_{sat}$; an undersaturated solution implies that $C_\infty < C_{sat}$ and $P_\infty > P_{sat}$, whereas in an equilibrated or saturated solution, $C_\infty = C_{sat}$ and $P_\infty = P_{sat}$.

As a concluding remark, it is worth mentioning that the pressure in the bubble will generally be higher than the ambient liquid pressure, $P_g(t) > P_\infty(t)$, due to the Laplace pressure that arises from the surface tension of the curved bubble interface. In fact, upon imposing $\dot{R} = \ddot{R} = J = \dot{J} = 0$ in the Rayleigh–Plesset equation (1.1), we obtain the equilibrium equation for the bubble surface,

$$P_g = P_\infty + \frac{2\gamma_{lg}}{R}. \tag{1.8}$$

The second term in the right-hand side is indeed the Laplace pressure of a spherical bubble of radius R. This implies that the interfacial concentration is always greater than the saturation concentration at the ambient pressure, $C_s(t) > C_{sat}$. In other words, surface tension drives bubbles to dissolve in saturated solutions under constant ambient pressures. This is the reason why after we pour a glass of water and wait for some seconds, we hardly see any bubbles remaining, even though the water is saturated with air.

1.3   Quasi-static, cavitating and translating bubbles

Not every mass transfer problem concerning bubbles can be modelled as spherically symmetric. Every scenario is governed by a particular set of geometrical and physical parameters, namely those that influence most the spatio-temporal evolution of the concentration field of dissolved gas surrounding the bubble(s). These can be substantially different depending on the problem. Logically, the growth or dissolution behaviour and dynamics will differ as much. For the case of growth, the increase of the bubble radius scales as $\Delta R \sim t$ in a train of rising champagne bubbles (Liger-Belair, 2005), whereas in

foaming beer, the apparent radius of the bubble-laden self-accelerating plumes scales as t^2 (Rodríguez-Rodríguez *et al.*, 2014). Hydrogen bubbles generated at microelectrodes grow as $t^{1/3}$ (Yang *et al.*, 2015) before detachment. Oxygen bubbles growing on a horizontal substrate in an uniformly supsersaturated solution follow $\Delta R \sim t^2$ (Verhaart *et al.*, 1979) while CO_2 bubbles growing in similar conditions are observed to quickly deviate from this scaling due to the onset of natural convection (Enríquez *et al.*, 2014). It is evident that the translational kinematics of spherical bubbles plays a critical role in the growth dynamics. Geometrical factors, from the mere presence of a wall to heavy confinement in porous media, gravity, and collective effects (bubble–bubble interactions) can be as important.

Thus, in an effort to situate the framework of the present thesis and reveal the cohesion of its contents, we have discerned three main categories of bubble mass transfer processes according to the kinematics of the gas bubble. These are (*a*) quasi-static bubbles, (*b*) cavitation or pulsating bubbles, and (*c*) translating bubbles. Figure 1.1 shows three tree diagrams relating these categories with their subcategories and some typical applications and scenarios in which they may be encountered.

Quasi-static and diffusion-driven bubbles

Category (*a*) encompasses the growth or dissolution of gas bubbles under quasi-static conditions. The term 'quasi-static' loosely describes the condition under which advection effects contribute poorly to the the rate of growth or dissolution of the bubble. A more precise description is that the flow velocity field relative to the non-stationary bubble interface is sufficiently small so that the advection term in the transport equation of the gas species (i.e. the advection–diffusion equation) has a secondary contribution (non-dominant but nonetheless present) on the rate of mass transfer across the bubble interface at all times.

The quasi-static condition can be assessed through two definitions of the Péclect number. The translation-based Péclet number must satisfy

$$Pe_t = \frac{UR}{D} \lesssim 1 \tag{1.9}$$

for diffusion to dominate over advection. Here, R is the bubble radius or an equivalent length, and D is the coefficient of diffusion. The characteristic velocity U is the far-field or mean flow velocity relative to the bubble centre. For the case of microbubbles convected along a microchannel, the characteristic velocity is better described by the shear velocity, $U = VR/H$, where V is the mean flow velocity in the lab reference frame and H is the relevant cross-sectional length of the channel (Shim *et al.*, 2014). Similarly, a second restriction is that the the boundary-based Péclet number (i.e. based on the velocity of expansion or contraction of the bubble boundary, typically $\dot{R}$) must likewise be small,

$$Pe_b = \frac{\dot{R}R}{D} \lesssim 1. \tag{1.10}$$

For sessile spherical (cap) bubbles adhered to surfaces, it is evident that first condition is redundant, since the bubble centre must move with a similar velocity as that of the expanding or shrinking interface, $U \sim \dot{R}$.

Returning now to figure 1.1, it can be seen that quasi-static bubbles have been further subdivided into production-controlled, diffusion-controlled and confinement-controlled

(a) Quasi-static bubbles

Production-controlled

Diffusion-controlled

Confinement-controlled

- In gas-evolving microelectrodes
- In laser-irradiated plasmonic nanoparticles or photo-electrodes

- Surface bubbles in liquids and carbonated beverages
- Surface nanobubbles
- In gas-evolving electrodes of water-splitting cells & electrochemical reactors
- (Parasitic) bubbles in microfluidics devices and Hele-Shaw cells
- Bubble clouds in microgravity
- In blood vessels and tissues, gels and viscoelastic materials
- In volcanic magmas & polymer melts

- **Porous media**
- CO_2 sequestration
- Solution gas-drive for oil production
- In magma chambers
- Supersaturated water injection

(b) Cavitation bubbles

Acoustic cavitation

Boiling

Rectified diffusion (gas-containing bubbles)

- Sonoluminescence
- Biomedicine: ultrasound contrast agents, drug delivery, sonoporation, tissue ablation
- Sonochemistry and ultrasonic cleaning
- Degradation of turbomachinery and hydraulic systems
- Acoustic streaming

- Nucleate and pool boiling
- Microbubble actuator and pumps
- Inkjet printing

(c) Translating bubbles

Buoyant bubbles

Microchannel flow

- Bubble trains in carbonated beverages and gas-evolving electrodes
- Bubble swarms in bubble column reactors
- Bubble plumes in tapped beer, and in limnic and volcanic eruptions

- **Microfluidics**, including generation of encapsulated microbubbles, solvent testing and chemical reactions and fuel cells
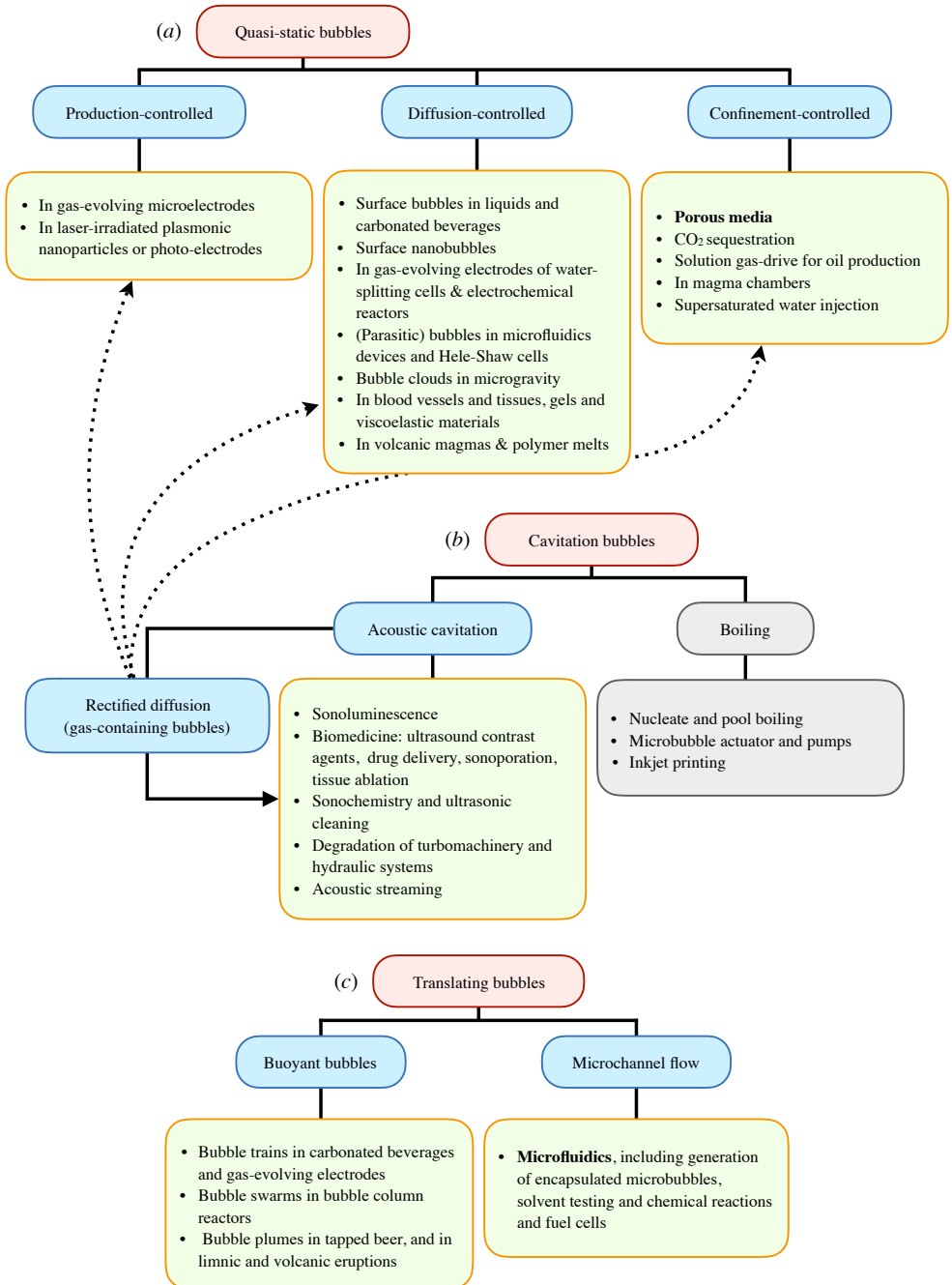
FIGURE 1.1. Tree diagrams categorizing some relevant scenarios of gas mass transfer concerning (a) quasi-static bubbles, (b) cavitation bubbles and (c) translating bubbles. The grey colour indicates that gaseous (non-vaporous) mass transfer is negligible in boiling bubbles.

bubbles. As one may have guessed from the thesis title, the work in this thesis evolves around the subcategory encompassing the diffusion-controlled growth and dissolution of quasi-static bubbles.

The term 'diffusion-driven' or 'diffusion-controlled' denotes that mass transfer is governed by the solute diffusion in the surrounding bulk liquid – advective, inertial, thermal or buoyancy-related effects play a secondary or negligible role. In mildly supersaturated liquid solutions, diffusion dictates the growth behaviour of bubbles growing on substrates (Barker *et al.*, 2002; Enríquez *et al.*, 2014; Moreno Soto *et al.*, 2017), bubbles growing on electrodes during electrolysis (Glas & Westwater, 1964; Brussieux *et al.*, 2011), surface nanobubbles (Lohse & Zhang, 2015), or bubble clouds in microgravity conditions (Vega-Martínez *et al.*, 2017). Diffusion-driven growth is also observed in bubbles trapped in supersaturated viscoelastic gelatin gels (Hamaguchi & Ando, 2015) and rhyolitic melts (Liu & Zhang, 2000). It then comes as no surprise that the dissolution of sessile bubbles (Kentish *et al.*, 2006; Kapodistrias & Dahl, 2012), microbubbles convected along microchannels at sufficiently low speeds (Shim *et al.*, 2014) and slowly rising antibubbles (Scheid *et al.*, 2014) are all dominated by diffusion.

The remaining types of bubbles mostly fall outside the scope of this work. Nonetheless, for the sake of completeness, we feel compelled to discuss them briefly in the next paragraphs.

Other types of bubbles

Production-controlled bubbles are those found growing on microelectrodes (Yang *et al.*, 2015), and laser-irradiated photoelectrodes or substrate impregnated with plasmonic nanoparticles (Wang *et al.*, 2017). The mass rate of solute gas into the bubble the bubble mass is proportional to the chemical reaction rate or the rate of plasmonic heating induced by the incident laser beam. A small localised liquid region in the immediate vicinity of the microelectrode or heated surface becomes supersaturated with gas, all of which desorps directly into the bubble.

Confinement-controlled bubbles are those found in porous media. These can be trapped during CO_2 sequestration (Buchgraber *et al.*, 2012), or may emerge and grow during oxygen-supersaturated water injection for bioremediation (Fry *et al.*, 1997) and depressurization through solution gas-drive (Akin & Kovscek, 2002). Growth of gas clusters in porous media is characterized by a pressurization step, where mass influx into the trapped bubble causes an increase of the the gas pressure whereas its volume remains fairly constant (Li & Yortsos, 1995). After exceeding a threshold pressure, the gas invades an adjacent pore. Experimental (Dominguez *et al.*, 2000) and theoretical studies involving network pore models (Li & Yortsos, 1995; Zhao & Ioannidis, 2011) establish that capillary and buoyancy forces govern the pattern formation of gas-occupied pores. Experiments show that the dissolution dynamics of bubbles in porous media can be quite complex, with bubble snapping, pinning and sweeping events (Buchgraber *et al.*, 2012).

The category of (*b*) cavitation bubbles can be subdivided into boiling bubbles and and acoustic cavitation bubbles. The first type are vapour bubbles, found for instance in boiling heat transfer (Dhir, 1998), whose rapid growth is dominated by thermal effects and the mass diffusion of gases is negligible in comparison (Plesset & Prosperetti, 1977). The second type refers to pulsating (usually gas-containing) bubbles driven by an oscillating acoustic pressure field, typically at ultrasonic frequencies in the kHz range as to trigger resonance.

Acoustic cavitation bubbles range from stable bubbles undergoing linear oscillations to inertial cavitation bubbles characterized by the periodic collapse of their vapour content. Inertial cavitation has many applications including noninvasive therapy and drug delivery (Coussios & Roy, 2008), sonochemistry (Fernandez Rivas *et al.*, 2010) and ultrasound cleaning (Verhaagen & Fernandez Rivas, 2016). Remarkably, the volumetric oscillations of the bubble can enhance the rate gas inflow into the bubble by a mechanism known as rectified mass diffusion (Hsieh & Plesset, 1961; Plesset & Prosperetti, 1977; Crum & Hansen, 1982). At high driving frequencies, the Péclet number based on the boundary velocity is likely to be large, $Pe_b \gg 1$. Hence, boundary-induced advection [cf. the advection term in (1.5)] is prone to play a decisive role in the mass transfer problem. In fact, every expansion–compression cycle induces a minute extra flux into the bubble due to the asymmetry of the mass transfer problem. Provided that the pressure forcing amplitude is large enough, bubbles may grow in saturated or even undersaturated solutions through the action of many cycles (Crum, 1980). Rectified diffusion is in fact responsible for the diffusive stability regime observed during single bubble sonoluminscence (Brenner *et al.*, 2002), where, notably, the surrounding water must be degassed to around 20 % of its saturation concentration of air. The dashed arrows in Figure 1.1 symbolize the fact that rectified diffusion can occur, by means of sonication, in many of the scenarios where quasi-static bubbles are encountered, such as in confined microreactors (Iida *et al.*, 2007), gels (Hamaguchi & Ando, 2015), or magma-filled pores in volcanic systems (Ichihara & Brodsky, 2006).

Lastly, we shift attention to category (*c*) concerning gas bubbles undergoing translation, and whose Péclet number is characteristicly large, $Pe_t \gg 1$. We begin with the subclass of buoyant bubbles. At large Reynolds and Péclet numbers, mass transfer mainly takes place within a very thin concentration boundary layer surrounding top surface of these buoyant bubbles (Figueroa-Espinoza & Legendre, 2010). The dissolution of single rising spherical bubbles (Takemura & Yabe, 1998), large Taylor bubbles (Aoki *et al.*, 2015), or homogenous swarms (Colombet *et al.*, 2015) are the essence of many mass transfer industrial processes. In beer, we may observe from single rising growing bubbles (Shafer & Zare, 1991), to buoyant plumes densely packed with bubbles (Rodríguez-Rodríguez *et al.*, 2014). In the latter, collective effects induce an autocatalytic growth effect that explains the violent CO_2-driven eruptions in certain lakes (Zhang & Kling, 2006).

The second subclass essentially consists in the dissolution of microbubbles along microchannels. The dissolution of bubbles in microfluidic systems is a topic that has gained much interest over the last years. A particular focus has been given to CO_2 bubbles (Abolhasani *et al.*, 2014), which have direct applications in microchemical systems and carbon capture. We may differentiate between segmented slug flow (Yue *et al.*, 2007; Sun & Cubaud, 2011; Yao *et al.*, 2017) and the bubbly flow regime (Cubaud *et al.*, 2012; Mikaelian *et al.*, 2015).

In most cases of (*c*), mass transfer is typically quantified by a Sherwood number, $Sh = 2Rk/D$, where k is the mass transfer coefficient. The Sherwood number is often empirically correlated to a combination of the Péclet, Reynolds and Schmidt numbers, gas volume fraction, or other control parameters of the system.

1.4   Diffusion-driven bubbles and the Epstein–Plesset equation

Before briefly outlining the work of this thesis, we feel impelled to comment on three fundamental assumptions and one rather special equation that exhaustively appear in the study and modelling of diffusion-driven bubble dynamics. Much of the theoretical treatment in this work is no exception to them.

Firstly, the interface of these bubbles, whether spherical or not, can be safely assumed to be in mechanical equilibrium at all times. The typical size and interface velocity of our diffusion-driven bubbles are $R \sim 10^{-4}$ m and $\dot{R} \sim 10^{-5}$ m/s. In fact, after a simple order of magnitude analysis on the Rayleigh–Plesset equation (1.1) we obtain [†]

$$P_g = P_\infty + \frac{2\gamma_{lg}}{R}, \tag{1.11}$$

where the neglected terms are at least four orders of magnitude less than the Laplace pressure term. Note that the Laplace pressure term can even be neglected for the case of large (e.g. mm-sized) bubbles.

The second assumption is that the bubble grows and dissolves isothermally i.e. the bubble has the same temperature as the ambient temperature of the liquid, T_∞, at all times. This is valid since the interface velocity is much slower than the thermal velocity, i.e. the heat-transfer Péclet number satisfies $\dot{R}R/D_{th} \ll 1$, where D_{th} is the thermal diffusivity of the liquid.

Thirdly, the gas contents are described by the equation of state of an ideal gas,

$$P_g = \rho_g R_g T_\infty \tag{1.12}$$

where R_g is the specific gas constant. In the case of multiple species, these are treated as a mixture of ideal gases and as such they comply with Dalton's Law.

The theory which undisputably represents the theoretical basis of a vast number of treatments on diffusion-driven growth – including the ones given in thesis – is the celebrated Epstein–Plesset equation (Epstein & Plesset, 1950). As such, it deserves a suiting introduction. The Epstein–Plesset equation is an approximate analytical differential equation for the radius dynamics of a bubble under the assumption of spherical symmetry (the bubble is fixed in an unbound liquid absent of body forces) together with the three assumptions just stated and under constant pressure. Moreover, the bubble has a finite initial size and the concentration field is initially uniform and equal to the far-field concentration C_∞.

They first solve the diffusion equation (1.5) without the advection term, $U(r, t) = 0$ and assume fixed, time-invariant boundary conditions at the interface $C(R, t) = k_H P_g$ together with $C(\infty, t) = C(r, 0) = C_\infty$. We stress that R and P_g are treated as constants – this simplification was later labelled as the quasi-static or quasi-stationary radius approximation (Weinberg & Subramanian, 1980). The resulting analytical expression for the interfacial concentration gradient can then be introduced into the mass balance equation given by equating (1.3) and (1.4). Making use of (1.11) and (1.12) to remove ρ_g from the expression,

---

[†] To do so, we take the gas density at $P_g \sim P_\infty \sim 10^5$ Pa to be $\rho_g \sim 1$ kg/m^3; the mass flux is therefore $J \sim \dot{R}^3 \rho_g / R^2 \sim 10^{-7}$ kg m^{-2} s^{-1}. The liquid density and viscosity are $\rho_l \sim 10^3$ kg/m^3 and $\mu \sim 10^{-3}$ kg m^{-1} s^{-1}; the surface tension is $\gamma_{sl} \sim 10^{-1}$ N/m.

we arrive to the father of all equations for the radius dynamics of quasi-static bubbles. The Epstein–Plesset equation is obtained:

$$\frac{\mathrm{d}R}{\mathrm{d}t} = -D\left(\frac{R_g T_\infty}{P_\infty}\right)\frac{k_H(P_\infty + 2\gamma_{lg}/R) - C_\infty}{1 + 2\gamma_{lg}/(3R)}\left[\frac{1}{R} + \frac{1}{\sqrt{\pi D t}}\right]. \tag{1.13}$$

1.5   Thesis outline

This thesis provides a fundamental study of four particular scenarios of diffusion-driven growth and dissolution of quasi-static bubbles. In § 2, we investigate the dissolution of a CO_2 spherical cap bubble in water adhered to a flat substrate. In the theoretical side, we extend the Epstien–Plesset solution in order to account for multiple species, the hindering effect of the wall and the contact line dynamics. In § 3 we provide a theoretical treatment of the so-called history effect, which is simply the naturally-occuring contribution of any past mass transfer events on the current mass flux across the bubble. This work continues in § 4, where we show the history effect experimentally for the case of a CO_2 spherical bubble tangent to a flat plate. We quantify numerically the effect of boundary-induced advection, and density-induced convection. Next, in § 5 we return to the fundamental problem of a CO_2 bubble dissolving in water but this time confined in a Hele-Shaw cell. We give special attention to the propagation of the radial CO_2 field which is visualized by means of planar laser-induced fluorescence. Finally, in § 6, we study a succession of hydrogen bubbles growing on flat electrodes under constant-current electrolysis. Their growth dynamics is compared with that of CO_2 bubbles growing in uniformly carbonated water.

As a final remark, one must take care with the nomenclature, since, truth be told, it is not consistent from one chapter to another. This should not pose much of a problem considering that all the chapters in this thesis are entirely self-contained. Looking back, we feel that some contents, especially in § 2, could have been somewhat improved. But, of course, it was not possible to know back then what we know now. Thus, we chose to leave everything as it was as a fond reminder of the learning curve we are all going through. A learning curve whose angle definitely became "much greater than zero" at some point.

We apologize for this in advance.

References

ABOLHASANI, M., GÜNTHER, A. & KUMACHEVA, E. 2014 Microfluidic studies of carbon dioxide. *Angew. Chem. Int. Edit.* **53** (31), 7992–8002.

AKIN, S. & KOVSCEK, A. R. 2002 Heavy-oil solution gas drive: a laboratory study. *J. Petrol. Sci. Eng.* **35** (1), 33–48.

AOKI, J., HAYASHI, K. & TOMIYAMA, A. 2015 Mass transfer from single carbon dioxide bubbles in contaminated water in a vertical pipe. *Int. J Heat Mass Tran.* **83**, 652–658.

BARKER, G. S., JEFFERSON, B. & JUDD, S. J. 2002 The control of bubble size in carbonated beverages. *Chem. Engng Sci.* **57** (4), 565–573.

BIRKHOFF, G., MARGULIES, R. S. & HORNING, W. A. 1958 Spherical bubble growth. *Phys. Fluids* **1** (3), 201–204.

BRENNER, M. P., HILGENFELDT, S. & LOHSE, D. 2002 Single-bubble sonoluminescence. *Rev. Mod. Phys.* **74**, 425–484.

BRUSSIEUX, C., VIERS, P., ROUSTAN, H. & RAKIB, M. 2011 Controlled electrochemical gas bubble release from electrodes entirely and partially covered with hydrophobic materials. *Electrochim. Acta* **56** (20), 7194–7201.

BUCHGRABER, M., KOVSCEK, A. R. & CASTANIER, L. M. 2012 A study of microscale gas trapping using etched silicon micromodels. *Transport Porous Med.* **95** (3), 647–668.

CARLTON, J. S. 2012 Chapter 9 – Cavitation. In *Marine Propellers and Propulsion*, 3rd edn., pp. 209 – 250. Oxford: Butterworth-Heinemann.

CHANDRAN, P., BAKSHI, S. & CHATTERJEE, D. 2015 Study on the characteristics of hydrogen bubble formation and its transport during electrolysis of water. *Chem. Eng. Sci.* **138**, 99–109.

COLOMBET, D., LEGENDRE, D., RISSO, F., COCKX, A. & GUIRAUD, P. 2015 Dynamics and mass transfer of rising bubbles in a homogenous swarm at large gas volume fraction. *J. Fluid Mech.* **763**, 254–285.

COUDER, YVES 2012 The fragmentation of the ocean: spray formation. *J. Fluid Mech.* **696**, 1–4.

COUSSIOS, C. C. & ROY, R. A. 2008 Applications of acoustics and cavitation to noninvasive therapy and drug delivery. *Annu. Rev. Fluid Mech.* **40** (1), 395–420.

CRUM, L. A. 1980 Measurements of the growth of air bubbles by rectified diffusion. *J. Acoust. Soc. Am.* **68**, 203–211.

CRUM, L. A. & HANSEN, G. M. 1982 Generalized equations for rectified diffusion. *J. Acoust. Soc. Am.* **72**, 1586–1592.

CUBAUD, T., SAUZADE, M. & SUN, R. 2012 CO_2 dissolution in water using long serpentine microchannels. *Biomicrofluidics* **6** (2), 022002.

DHIR, V. K. 1998 Boiling heat transfer. *Annu. Rev. Fluid Mech.* **30** (1), 365–401.

DOMINGUEZ, A., BORIES, S. & PRAT, M. 2000 Gas cluster growth by solute diffusion in porous media. Experiments and automaton simulation on pore network. *Int. J. Multiphase Flow* **26** (12), 1951 – 1979.

ENRÍQUEZ, O. R., SUN, C., LOHSE, D., PROSPERETTI, A. & VAN DER MEER, D. 2014 The quasi-static growth of CO_2 bubbles. *J. Fluid Mech.* **741** (R1).

EPSTEIN, P. S. & PLESSET, M. S. 1950 On the stability of gas bubbles in liquid—gas solutions. *J. Chem. Phys.* **18** (11), 1505–1509.

FERNANDEZ RIVAS, D., PROSPERETTI, A., ZIJLSTRA, A. G., LOHSE, D. & GARDENIERS, H. J. G. E. 2010 Efficient sonochemistry through microbubbles generated with micromachined surfaces. *Angew. Chem. Int. Edit.* **49** (50), 9699–9701.

FIGUEROA-ESPINOZA, B. & LEGENDRE, D. 2010 Mass or heat transfer from spheroidal gas bubbles rising through a stationary liquid. *Chem. Eng. Sci.* **65** (23), 6296 – 6309.

FRY, V. A., SELKER, J. S. & GORELICK, S. M. 1997 Experimental investigations for trapping oxygen gas in saturated porous media for in situ bioremediation. *Water Resour. Res.* **33** (12), 2687–2696.

FUSTER, D. & MONTEL, F. 2015 Mass transfer effects on linear wave propagation in diluted bubbly liquids. *J. Fluid Mech.* **779**, 598–621.

GLAS, J. P. & WESTWATER, J. W. 1964 Measurements of the growth of electrolytic bubbles. *Int. J. Heat Mass Transfer* **7**, 1427–1443.

HAMAGUCHI, F. & ANDO, F. 2015 Linear oscillation of gas bubbles in a viscoelastic material under ultrasound irradiation. *Phys. Fluids* **27** (11).

HASZELDINE, R. S. 2009 Carbon capture and storage: How green can black be? *Science* **325** (5948), 1647–1652.

HSIEH, D.-Y. 1965 Some analytical aspects of bubble dynamics. *J. Basic Eng.* **87**, 991–1005.

HSIEH, D.-Y. & PLESSET, M. S. 1961 Theory of rectified diffusion of mass into gas bubbles. *J. Acoust. Soc. Am.* **33** (2), 206–215.

ICHIHARA, M. & BRODSKY, E. E. 2006 A limit on the effect of rectified diffusion in volcanic systems. *Geophys. Res. Lett.* **33** (2), L02316.

IIDA, Y., TUZIUTI, T., YASUI, K., TOWATA, A. & KOZUKA, T. 2007 Bubble motions confined in a microspace observed with stroboscopic technique. *Ultrason. Sonochem.* **14** (5), 621 – 626.

JONES, O. C. & ZUBER, N. 1978 Bubble growth in variable pressure fields. *J. Heat. Trans.* **100** (3), 453–459.

KANTARCI, N., BORAK, F. & ULGEN, K. O. 2005 Bubble column reactors. *Process Biochem.* **40** (7), 2263 – 2283.

KAPODISTRIAS, G. & DAHL, P. H. 2012 Scattering measurements from a dissolving bubble. *J. Acoust. Soc. Am.* **131** (6), 4243–4251.

KENTISH, S., LEE, J., DAVIDSON, M. & ASHOKKUMAR, M. 2006 The dissolution of a stationary spherical bubble beneath a flat plate. *Chem. Engng Sci.* **61** (23), 7697–7705.

KONTOPOULOU, M. & VLACHOPOULOS, J. 1999 Bubble dissolution in molten polymers and its role in rotational molding. *Polym. Eng. Sci.* **39** (7), 1189–1198.

LI, X. & YORTSOS, Y. C. 1995 Theory of multiple bubble growth in porous media by solute diffusion. *Chem. Eng. Sci.* **50** (8), 1247 –1271.

LIGER-BELAIR, G. 2005 The physics and chemistry behind the bubbling properties of champagne and sparkling wines: A state-of-the-art review. *J. Agric. Food Chem.* **53** (8), 2788–2802.

LIU, Y. & ZHANG, Y. 2000 Bubble growth in rhyolitic melt. *Earth Planet. Sci. Lett.* **181** (1), 251 – 264.

LOHSE, D. & ZHANG, X. 2015 Surface nanobubbles and nanodroplets. *Rev. Mod. Phys.* **87**, 981–1035.

MANGAN, M., MASTIN, L. & SISSON, T. 2004 Gas evolution in eruptive conduits: combining insights from high temperature and pressure decompression experiments with steady-state flow modeling. *J. Volcanol. Geotherm. Res.* **129** (1), 23 – 36, the role of laboratory experiments in volcanology.

DE MAS, N., GÜNTHER, A., SCHMIDT, M. A. & JENSEN, K. F. 2003 Microfabricated multiphase reactors for the selective direct fluorination of aromatics. *Ind. Eng. Chem. Res.* **42** (4), 698–710.

MIKAELIAN, D., HAUT, B. & SCHEID, B. 2015 Bubbly flow and gas–liquid mass transfer in square and circular microchannels for stress-free and rigid interfaces: dissolution model. *Microfluid. Nanofluid.* **19** (4), 899–911.

MORENO SOTO, Á., PROSPERETTI, A., LOHSE, D. & VAN DER MEER, D. 2017 Gas depletion through single gas bubble diffusive growth and its effect on subsequent bubbles. *J. Fluid Mech. (in press)* .

PAPADOPOULOU, V., ECKERSLEY, R. J., BALESTRA, C., KARAPANTSIOS, T. D. & TANG, M.-X. 2013 A critical review of physiological bubble formation in hyperbaric decompression. *Adv. Colloid Interface Sci.* **191**, 22 – 30.

PARK, J. I., JAGADEESAN, D., WILLIAMS, R., OAKDEN, W., CHUNG, S., STANISZ, G. J. & KUMACHEVA, E. 2010 Microbubbles loaded with nanoparticles: A route to multiple imaging modalities. *ACS Nano* **4** (11), 6579–6586.

PAYVAR, P. 1987 Mass transfer-controlled bubble growth during rapid decompression of a liquid. *Int. J. Heat Mass Transfer* **30** (4), 699–706.

PLESSET, M. S. & PROSPERETTI, A. 1977 Bubble dynamics and cavitation. *Annu. Rev. Fluid Mech* **9** (1), 145–185.

PLESSET, M. S. & ZWICK, S. A. 1954 The growth of vapor bubbles in superheated liquids. *J. Applied Phys.* **25** (4), 493–450.

PROSPERETTI, A. 1982 A generalization of the rayleigh–plesset equation of bubble dynamics. *Phys. Fluids* **25** (3), 409–410.

PROSPERETTI, A., CRUM, L. A. & COMMANDER, K. W. 1988 Nonlinear bubble dynamics. *J. Acoust. Soc. Am.* **83** (2), 502–514.

RODRÍGUEZ-RODRÍGUEZ, J., CASADO-CHACÓN, A. & FUSTER, D. 2014 Physics of beer tapping. *Phys. Rev. Lett.* **113**, 214501.

SCHEID, B., ZAWALA, J. & DORBOLO, S. 2014 Gas dissolution in antibubble dynamics. *Soft Matter* **10**, 7096–7102.

SCRIVEN, L. E. 1959 On the dynamics of phase growth. *Chem. Eng. Sci.* **10**, 1–13.

SHAFER, N. E. & ZARE, R. N. 1991 Through a beer glass darkly. *Physics Today* **44** (10), 48–52.

SHIM, S., WAN, J., HILGENFELDT, S., PANCHAL, P. D. & STONE, H. A. 2014 Dissolution without disappearing: multicomponent gas exchange for CO_2 bubbles in a microfluidic channel. *Lab Chip* **14**, 2428–2436.

SHPAK, O., STRICKER, L., VERSLUIS, M. & LOHSE, D. 2013 The role of gas in ultrasonically driven vapor bubble growth. *Phys. Med. Biol.* **58** (8), 2523.

SUN, R. & CUBAUD, T. 2011 Dissolution of carbon dioxide bubbles and microfluidic multiphase flows. *Lab Chip* **11** (17), 2924–2928.

TAKEMURA, F. & YABE, A. 1998 Gas dissolution process of spherical rising gas bubbles. *Chem. Eng. Sci.* **53** (15), 2691–2699.

VEGA-MARTÍNEZ, P., RODRÍGUEZ-RODRÍGUEZ, J., VAN DER MEER, D. & SPERL, M. 2017 Drop tower setup to study the diffusion-driven growth of a foam ball in supersaturated liquids in microgravity conditions. *Microgravity Science and Technology* **29** (4), 297–304.

VERHAAGEN, B. & FERNANDEZ RIVAS, D. 2016 Measuring cavitation and its cleaning effect. *Ultrason. Sonochem.* **29**, 619 – 628.

VERHAART, H. F. A., DE JONGE, R. M. & VAN STRALEN, S. J. D. 1979 Growth rate of a gas bubble during electrolysis in supersaturated liquid. *Int. J. Heat Mass Transfer* **23**, 293–299.

VOLK, A., ROSSI, M., KAHLER, C. J., HILGENFELDT, S. & MARIN, A. 2015 Growth control of sessile microbubbles in pdms devices. *Lab Chip* **15**, 4607–4613.

WANG, Y., ZAYTSEV, M. E., THE, H. L., EIJKEL, J. C. T., ZANDVLIET, H. J. W., ZHANG, X. & LOHSE, D. 2017 Vapor and gas–bubble growth dynamics around laser-irradiated, water-immersed plasmonic nanoparticles. *ACS Nano* **11** (2), 2045–2051.

WEINBERG, M. C. & SUBRAMANIAN, R. S. 1980 Dissolution of multicomponent bubbles. *J. Am. Ceram. Soc.* **63** (9-10), 527–531.

YANG, X., KARNBACH, F., UHLEMANN, M., ODENBACH, S. & ECKERT, K. 2015 Dynamics of single hydrogen bubbles at a platinum microelectrode. *Langmuir* **31** (29), 8184–8193.

YAO, C., LIU, Y., ZHAO, S., DONG, Z. & CHEN, G. 2017 Bubble/droplet formation and mass transfer during gas–liquid–liquid segmented flow with soluble gas in a microchannel. *AIChE J.* **63** (5), 1727–1739.

YUE, J., CHEN, G., YUAN, Q., LUO, L. & GONTHIER, Y. 2007 Hydrodynamics and mass transfer characteristics in gas–liquid flow through a rectangular microchannel. *Chem. Eng. Sci.* **62** (7), 2096–2108.

ZHANG, Y. & KLING, G. W. 2006 Dynamics of lake eruptions and possible ocean eruptions. *Annu. Rev. Earth Pl. Sc.* **34** (1), 293–324.

ZHAO, W. & IOANNIDIS, M. A. 2011 Gas exsolution and flow during supersaturated water injection in porous media: I. Pore network modeling. *Adv. Water Resour.* **34** (1), 2 – 14.

CHAPTER TWO

Peñas-López, P., Parrales, M. A. & Rodríguez-Rodríguez, J. 2015. Dissolution of a CO_2 spherical cap bubble adhered to a flat surface in air-saturated water. *J. Fluid Mech*. **775**, 53–76. URI: http://hdl.handle.net/10016/26898

CHAPTER THREE

Peñas-López, P., Parrales, M. A., Rodríguez-Rodríguez, J. & van der Meer, D. 2016. The history effect in bubble growth and dissolution. Part 1. Theory. *J. Fluid Mech*. **800**, 180–212. URI: http://hdl.handle.net/10016/26899

CHAPTER FOUR

Peñas-López, P., Moreno Soto, Á., Parrales, M. A., van der Meer, D., Lohse, D. & Rodríguez-Rodríguez, J. 2017b. The history effect on bubble growth and dissolution. Part 2. Experiments and simulations of a spherical bubble attached to a horizontal flat plate. *J. Fluid Mech*. **820**, 479–510.
URI: http://hdl.handle.net/10016/26907

CHAPTER FIVE

Peñas-López, P., van Elburg, B., Parrales, M. A. & Rodríguez-Rodríguez, J. 2017. Diffusion of dissolved CO_2 in water propagating from a cylindrical bubble in a horizontal
Hele-Shaw cell. *Phys. Rev. Fluids* **2**, 063602.
URI: http://hdl.handle.net/10016/26910

CHAPTER SIX

van der Linde, P., Moreno Soto, Á., Peñas-López, P., Rodríguez-Rodríguez, J., Lohse, D., Gardeniers, H., van der Meer, D. & Fernández Rivas, D. 2017[a]. Electrolysis-driven and pressure-controlled diffusive growth of successive bubbles on micro-structured surfaces. *Langmuir*, **33**(45), 12873–12886.
URI: http://hdl.handle.net/10016/26911

SEVEN

Conclusions

This thesis comprises the fundamental study of four distinct but closely related problems concerning the diffusion-driven dissolution and growth of quasi-static gas bubbles.

We began in § 2 by examining the dissolution of mm-sized CO_2 spherical cap bubbles (SCBs) immersed in air-saturated water and adhered to collagen-coated glass and PMMA substrates. The dissolution process is characterized by the simultaneous dominant outflow and modest inflow of CO_2 gas and air respectively. A quasi-equilibrium size is attained after a few minutes, as soon as the bubble is depleted of CO_2. Thereafter, the bubble is entirely composed of air and it slowly dissolves (the expected lifetime is of the order of days) purely due to the Laplace pressure. The liquid-phase contact angles of our SCBs were large, namely in the range between 30° and 90°. It was found that the quasi-static contact angle behaviour was well reproduced by a simplistic model based on adhesion hysteresis. We then presented a theoretical model for multicomponent SCBs based on the Epstein–Plesset solution. The model accounts for the contact angle dynamics and the hindering effect of the plate on mass transfer. Moreover, we developed a simulation based on finite differences in toroidal coordinates. The concentration field was explicitly solved for from the diffusion equation, confined to the real geometry and subject to the real boundary conditions. However, advection was not accounted for.

Chapters 3 and 4 are devoted to the study of the so-called history effect: namely the contribution of any past mass transfer events between a gas bubble and its liquid surroundings towards the current diffusion-driven bubble growth or dissolution dynamics. The history effect arises when the concentration of dissolved gas at the bubble surface, dictated by Henry's law, depends on time.

In § 3 we provided a theoretical treatment of the history effect under the assumptions of spherical symmetry and negligible advection. We showed that the contribution of the history effect in the current interfacial concentration gradient is fully contained within a memory integral (in nonlinear time) of the interfacial concentration. We then derived an analogous equation to the Epstein–Plesset equation for the bubble dynamics. This equation is not restricted to a constant-pressure time history and does not make use of the quasi-static radius approximation. It was then analytically solved for the case of multiple step-like jumps in pressure. Finally, we considered a non-inertial bubble that pulsates under harmonic pressure forcing in the limit of small amplitude oscillations. The history effect was shown to induce a phase shift in the interfacial concentration gradient with respect to the phase of the interfacial concentration, or equivalently the ambient pressure. This phase-shift was shown to always promote long-term growth.

In § 4 we performed experiments on isolated spherical CO_2 bubbles adhered to a flat plate in carbonated water. We showed that the mass of the bubble can experience transient growths even when the (non-uniform) pressure is kept above saturation at all times. Moreover, by subjecting the bubble to two consecutive identical expansion–compression cycles, we were able to observe how the history effect becomes manifest in a higher growth rate at the beginning of the second cycle. The experiments were reproduced numerically. The finite-difference numerical model for the concentration field employed in § 2 was reworked in tangent-sphere coordinates. The velocity field was similarly obtained through a vorticity–streamfunction method. The simulations allowed to discern the influence of boundary-induced advection and density-induced natural convection on the bubble dynamics, concentration field and flow structure.

Next, in § 5 we investigated the dissolution of a cylindrical CO_2 bubble confined in a horizontal Hele-Shaw cell dissolving in air-saturated water. We visualized, by means of planar laser-induced fluorescence, the boundary layer of dissolved CO_2 that propagates by diffusion from the dissolving bubble. Interestingly, the fluorescence intensity of sodium fluorescein was found to vary linearly with dissolved CO_2 concentration in the low-concentration region where pH $\gtrsim 5.5$. In the region closer to the bubble, where pH $\lesssim 5$, the intensity varied linearly with pH. The diffusion-driven transport of CO_2 was described by two simple analytical diffusion models and were then validated against numerical simulation which solved the full problem regarding a dissolving multicomponent bubble. Lastly, we derived an analogous Epstein–Plesset equation in cylindrical coordinates that was able to effectively predict the bubble dissolution rate. The differences between the model and the simulation were attributed to the fact that the model did not consider history effects. History effects are omnipresent in multicomponent bubbles since the partial pressure of each species, hence the interfacial concentrations, may undergo considerable variations as the bubble composition changes.

Finally, in § 6 we explored the growth dynamics of a succession of H_2 bubbles driven by constant-current electrolysis. The large surface area of the electrode upon which they grow ensured that the bubble growth was diffusion-controlled. The accumulation of dissolved H_2 near the gas-evolving electrode was hindered by several depletion sources, including depletion from previous bubbles in the succession. In fact, the depletion effect of the cavity opening where the electrode was held and of parasitic bubbles forming on the cavity sidewall were responsible for a notable retardation in growth as the bubbles approached their departure size. This effect could be quantified by simulations. The simulation in § 4 was in fact extended with the inclusion of a microlayer region subject to a non-zero flux boundary condition in order to account for the micropillar-on-the-electrode configuration in which the bubbles nucleate and grow. We concluded that the degree of supersaturation near the electrode, and consequently the bubble growth rates, were largely unsteady and prone to fluctuations. It is therefore erroneous to assume that the bubble growth rates will always be the same provided that the current density is constant, the most important reason being that the steady-state value of the supersaturation near the electrode is not attained immediately.

Acknowledgements

It takes two flints to make a fire.

– Louisa May Alcott (1832–1888)

First and foremost, I want to express my deepest gratitude towards my advisors, Javier Rodríguez and Miguel Ángel Parrales, both great scientists, but even better friends and colleagues. Thank you, Javier, for your constant encouragement, enthusiasm and guidance. Thank you, Miguel, for your patience and your invaluable teachings. You are both the best advisors I could have hoped for. I know I have not always been the easiest of people to work with. Regardless, your support has been unconditional. It has been an honour to be your student these last four years. I hope to continue learning from you for many years to come.

I want to continue by thanking everyone with whom I have had the pleasure to officially collaborate. In strict order of appearance, I thank Devaraj van der Meer, Álvaro Moreno Soto, Detlef Lohse, Benjamin van Elburg, David Fernández Rivas, Peter van der Linde and Han Gardeniers. They are all directly responsible, in one way or the other, for the better part of this thesis. I also thank Oscar Enríquez, whose previous work opened up the way for us, and with whom I am currently working. Interestingly enough, all of them belong – or did at some point – to the University of Twente, where I did a five-month research stay at the Physics of Fluids Group. I thank Álvaro, Devaraj, Detlef and José Encarnación for hosting me so kindly. I bear special gratitude to David and Peter for giving me the opportunity to work with them. I also seize this opportunity to give my thanks to the rest of the *Physics of Fluids* and *Mesoscale Chemical Systems* members with whom I had the pleasure to interact. A special thanks goes to Joanita Leferink for always accommodating me in the best possible way.

Moving on, I would like to acknowledge all the professors and staff of the *Departamento de Ingeniería Térmica y de Fluidos* (at UC3M) for always being so kind and friendly to me. I also want to thank all my colleagues for making these last four years such a memorable experience. I owe a very special thanks to Patricia Vega, soon-to-be collaborator, for her invaluable help and friendship. Another big thanks goes to my office (and indoor cycling) mates, Juan Sánchez Monreal and Paula Consoli. In this matter, I am grateful to Nacor Burgos, the cycling tutor at the university, for the few megapascals of negative mental strain, or rather pressure, that his merciless routines forced out of me every single time. As for the rest of colleagues, I give thanks, again in order of appearance, to Ana Medina, Elena Igualada, Pedro González, Luis Cutz, Daniel Moreno, Alberto Quintero, Daniel Gómez, Pablo García Salaberri, Daniel Martínez, María Fernández, Alejandro Martínez and Alejandro Millán, among many others.

This thesis is dedicated to my parents, Mariajosé and Gabriel. I owe you everything and I am very fortunate to have you. I also thank my brother Juan for standing me all these years.

I will not forget my old friends from Tres Cantos and thereabouts. In strict alphabetical order, I thank Bruno Belmonte, Marta Bermejo, John & Frank Lee, Carlos Franco, Alejandro Gómez, Erik Hinton, Rodrigo Málaga, Pio Monti and Clara Serena. Cheers for the good times spent and for always being there for me.

And lastly, a very special mention goes to Burçak Birben. Not so long ago, you burst into my life and unequivocally changed it, including me, for the best. You truly complete me. All I can say is thank you: *sen sadece benimsin, her şeyim.* You are my favourite bubble.